# 4    Results

## 4.1    CCR2-deficient CD8$^+$ T cells induce less graft-versus-host disease

The role of CCR2 expression on allogeneic donor CD8$^+$ T cells in the development of GVHD was examined in a well-described murine BMT model with a full MHC class I and II mismatch: B6 (H-2$^b$)→C3FeB6F1 (H-2$^{b/k}$). Although CD4$^+$ T cells are more potent in this strain combination, severe lethal GVHD can be initiated by CD8$^+$ T cells alone (142). Donor CD8$^+$ T cells were purified from B6 WT and CCR2$^{-/-}$ splenocytes by MACS separation and injected with TCD WT BM via the tail vein into lethally irradiated (1300 cGy) C3FeB6F1 hosts. This experimental setup allows the selective analysis of the effects of CCR2-deficiency on donor CD8$^+$ T cells without any confounding effects of CCR2-deficiency on host or BM-derived cells. Survival of transplanted mice was monitored daily for 15 weeks. In addition, mice were scored weekly for 5 clinical parameters associated with GVHD (weight loss, hunched posture, activity level, fur ruffling, and skin lesions) on a scale from 0 to 2 (Table 5) and a clinical GVHD score was generated by summation of these criteria (137).

As expected, no GVHD morbidity and mortality was observed for control mice, which received TCD WT BM alone (Figure 6A). Addition of WT CD8$^+$ T cells led to the development of severe acute GVHD (with diarrhea, skin damage, fur damage and hunched back), which resulted in high mortality rates and the survival of only 46.6% of BMT recipients by the end of the experiment. However, when CCR2$^{-/-}$ CD8$^+$ T cells were administered, mice exhibited a delayed development of GVHD and more than 80% of BMT recipients survived (Figure 6A). This survival advantage was statistically significant and corresponded to a significant decrease in clinical GVHD scores (3.8±0.36 for WT vs. 1.9±0.37 for CCR2$^{-/-}$ at the end of the experiment) (Figure 6B). In addition, weight loss, as a sign of diarrhea and intestinal GVHD, was significantly reduced in recipients of CCR2$^{-/-}$ CD8$^+$ T cells (Figure 6C). Differences between recipients of WT and CCR2$^{-/-}$ CD8$^+$ T cells became most prominent later than 9 weeks after BMT.

A delay of mortality of recipients of CCR2$^{-/-}$ CD8$^+$ T cells was also seen in a combined GVHD/GVT model, where B6D2F1 recipients were transplanted with TCD WT BM in combination with WT or CCR2$^{-/-}$ CD8$^+$ T cells plus P815 mastocytoma cells (Figure 17A). Autopsies and histopathological analysis demonstrated that this delay was mainly due to decreased GVHD mortality early after BMT (Figure 17B).

In summary, these results demonstrate that CCR2 is an important molecule for the induction of GVHD by CD8$^+$ donor T cells.
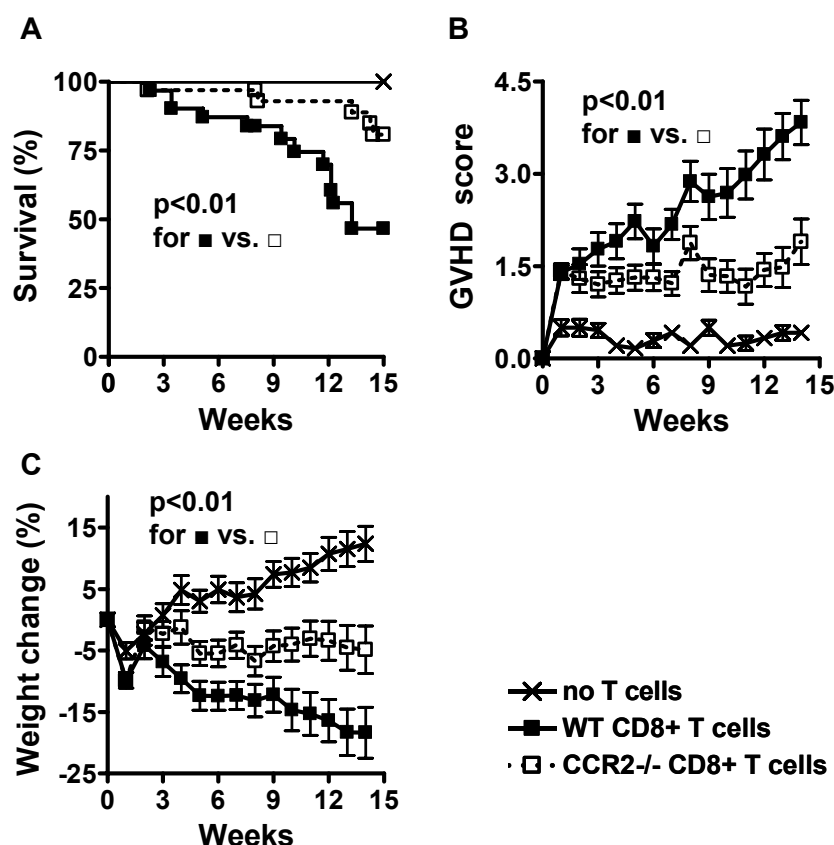
***Figure 6: CCR2^{-/-} CD8^+ T cells induce less GVHD morbidity and mortality than WT CD8^+ T cells.***
*Lethally irradiated (1300 cGy) C3FeB6F1 mice received 5x10^6 TCD WT BM cells alone (x, n=12) or in combination with 3-4.5x10^6 WT (■, n=31) or CCR2^{-/-} (□, n=33) CD8^+ T cells. Data represent three combined experiments. A) Kaplan-Meier survival curve. B) Clinical GVHD score (mean ± SEM). C) Weight curve (mean ± SEM).*

## 4.2    CCR2-deficient CD8^+ T cells induce less damage to the gut and liver

The pathological correlate of acute GVHD is the development of epithelial damage mainly in the gut, liver and skin (3). The histological features of acute GVHD in the gut are mainly characterized by villus blunting, lamina propria inflammation, crypt destruction and mucosal atrophy (143), whereas the histological features of acute GVHD in the liver consist of bile duct epithelial damage, cholestasis, endothelialitis and inflammatory cell infiltration into portal areas (144). In the skin, keratinocyte apoptosis, dyskeratosis, exocytosis of lymphocytes and dermal perivascular lymphocytic infiltration are characteristic signs (145) (Table 1).

To determine if the reduced morbidity and mortality of CCR2^{-/-} CD8^+ T cell recipients could be attributed to reduced damage to specific target organs and could therefore point towards a possible organ specificity of CCR2 in GVHD, histopathological analyses of small bowel, large

bowel, liver and skin were performed. Lethally irradiated C3FeB6F1 recipients were transplanted with TCD WT BM together with WT or CCR2$^{-/-}$ CD8$^{+}$ T cells and were monitored closely for the development of GVHD. Small and large bowel, liver and skin were taken at day 21 when only minimal clinical signs of GVHD were observable and at day 55 when most WT mice had already developed moderate GVHD and some WT mice had already died. Organs were fixed in formalin, paraffin-embedded, sectioned and stained with hematoxylin and eosin. Gut and liver histopathology was subsequently analyzed by C. Liu (University of Florida College of Medicine, Gainesville, FL) and a semiquantitative score consisting of 19 to 22 different parameters associated with GVHD was calculated (22). Skin samples were examined by G.F. Murphy (Harvard Medical School, Boston, MA) and the number of apoptotic cells/mm epidermis as a correlate for cutaneous GVHD was determined (138).

Recipients of CCR2$^{-/-}$ CD8$^{+}$ T cells developed significantly less histopathological damage of the large bowel at day 21 (11.3±1.1 for WT vs. 8.3±0.9 for CCR2$^{-/-}$) and of the small bowel (9.0±0.8 for WT vs. 4.5±0.8 for CCR2$^{-/-}$), large bowel (6.8±0.6 for WT vs. 3.9±0.7 for CCR2$^{-/-}$) and liver (13.6±1.3 for WT vs. 6.4±1.5 for CCR2$^{-/-}$) at day 55 (Figure 7A-C). These data correlate nicely with the observed reduction of mortality, clinical GVHD scores and weight loss in recipients of CCR2$^{-/-}$ CD8$^{+}$ T cells, which was more prominent at later time points.
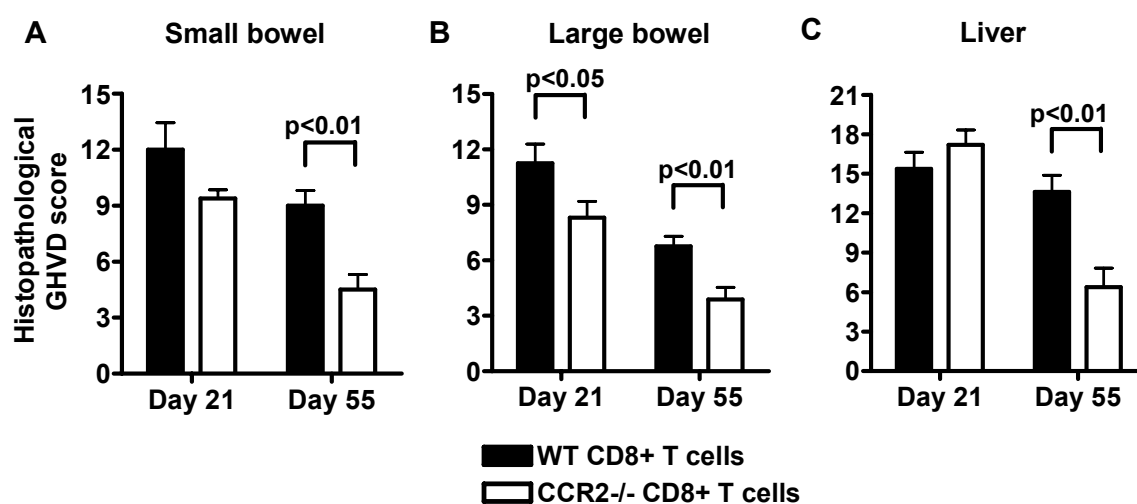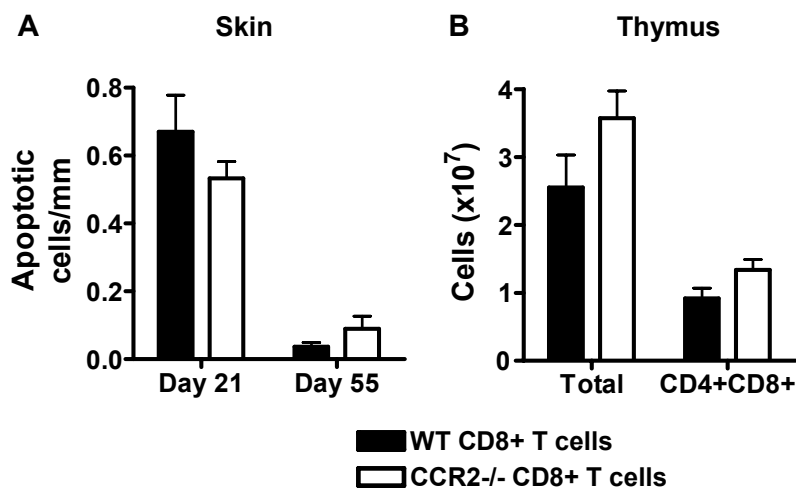


***Figure 7: CCR2$^{-/-}$ CD8$^{+}$ T cells cause less gut and liver damage than WT CD8$^{+}$ T cells.***
*Lethally irradiated (1300 cGy) C3FeB6F1 mice received 5x10$^{6}$ TCD WT BM cells in combination with 3-4.5x10$^{6}$ WT (■) or CCR2$^{-/-}$ (□) CD8$^{+}$ T cells. Organs were taken on day 21 and day 55. Hematoxylin and eosin-stained slides were analyzed and scored for histopathological damage. A) Small bowel. B) Large bowel. C) Liver. Shown is the mean ±SEM for 8-10 mice per group per time point.*

However, when skin pathology was analyzed, no significant differences for recipients of WT and CCR2$^{-/-}$ CD8$^+$ T cells were detected (Figure 8A). Notably, overall levels of skin damage were very low, suggesting that CD8$^+$ T cells are not sufficient to induce severe skin GVHD in this model.

Thymic dysfunction contributes to the profound immunodeficiency regularly observed after allogeneic HSCT (146). The pathological correlate of thymic dysfunction during GVHD is a change in thymic architecture and a decrease in overall thymic cellularity as well as a decrease in CD4/CD8 double positive thymocyte (CD4$^+$/CD8$^+$) counts (147). These changes occur as early as two weeks after transplantation and progress in the course of the disease. To determine if CCR2-deficiency has any influence on thymic damage, thymic cellularity and CD4$^+$CD8$^+$ counts were determined on day 21 after BMT. No significant differences were observed between recipients of WT and CCR2$^{-/-}$ CD8$^+$ T cells, suggesting that CCR2 is not relevant for the induction of thymic damage (Figure 8B).
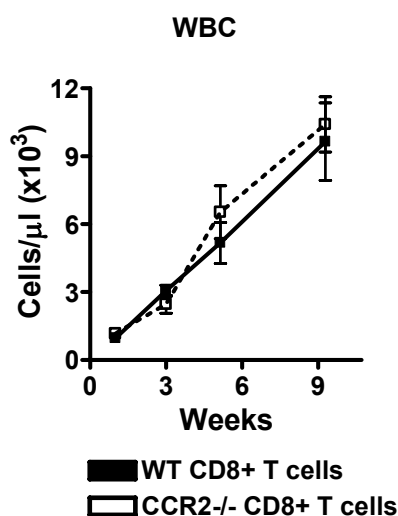


***Figure 8: Damage to skin and thymus is not reduced in CCR2$^{-/-}$ CD8$^+$ T cell recipients.***
*Lethally irradiated (1300 cGy) C3FeB6F1 mice received 5x10$^6$ TCD WT BM cells in combination with 3-4.5x10$^6$ WT (■) or CCR2$^{-/-}$ (□) CD8$^+$ T cells. A) Skin GHVD was determined on day 21 and day 55 by the number of apoptotic keratinocytes/mm epidermis. Shown is the mean ± SEM for 8-10 mice per group per time point. B) Total thymic cellularity and CD4$^+$CD8$^+$ thymocyte counts were determined by FACS on day 21. Shown is the mean ± SEM for 7 mice per group.*

Alloreactive donor CD8$^+$ T cells play a pivotal role in preventing allogeneic marrow graft rejection in mice (148). To assess the effects of CCR2-deficiency on recovery of white blood cells, red blood cells and platelets, complete blood counts (CBC) were determined 1, 3, 5 and 9

weeks after BMT. No significant differences were observed for total peripheral white blood cell counts and other CBC parameters (Figure 9 and data not shown).



**WBC**

*Figure 9: Engraftment is intact in CCR2<sup>-/-</sup> CD8<sup>+</sup> T cell recipients.*

*Lethally irradiated (1300 cGy) C3FeB6F1 mice received $5x10^6$ TCD WT BM cells in combination with $3 \ x10^6$ WT (■) or CCR2<sup>-/-</sup> (□) CD8<sup>+</sup> T cells. Peripheral blood was obtained at weeks 1, 3, 5 and 9 after BMT and CBCs were determined. Shown is the mean $\pm$ SEM for white blood cell (WBC) counts for 7-10 mice per group per time point.*

In summary, results from these analyses show that CCR2$^{-/-}$ CD8$^{+}$ T cells induce less GVHD-associated intestinal and liver damage, while damage to the skin and thymus is not reduced and the ability of CCR2$^{-/-}$ CD8$^{+}$ T cells to facilitate engraftment is not diminished. This demonstrates that CCR2$^{-/-}$ CD8$^{+}$ T cells have functional defects, which mediate organ specificity to the gut and liver, while they do not have a general decrease in alloreactivity.

## 4.3    CCR2-deficient CD8$^{+}$ T cells have a migratory defect to the gut and liver

The decreased GVHD morbidity and mortality and the decreased damage to the gut and liver in recipients of CCR2$^{-/-}$ CD8$^{+}$ T cells could be due to a migration defect of CCR2$^{-/-}$ CD8$^{+}$ T cells into these organs. To test this hypothesis, a competitive *in vivo* migration assay was performed. WT CD8$^{+}$ T cells expressing the congenic marker Thy1.1 and CCR2$^{-/-}$ CD8$^{+}$ T cells (Thy1.2) were positively selected by MACS, the post-selection purity was determined by FACS and equal numbers of both cell types were mixed ($2x10^6$ WT CD8$^{+}$ T cells plus $2x10^6$ CCR2$^{-/-}$ CD8$^{+}$ T cells). Accuracy of this procedure was determined by FACS analysis of Thy1.1 and Thy1.2 expression (Figure 10A). Mixed CD8$^{+}$ T cells and $5x10^6$ TCD WT BM cells (CD45.1) were subsequently transplanted in lethally irradiated C3FeB6F1 recipients. GVHD target organs (liver and small bowel) and secondary lymphoid organs (spleen, PP, PLN, MLN) were harvested on days 6, 14, and 28 after BMT and mononuclear cells were isolated. The percentage of infiltrating WT and CCR2$^{-/-}$ CD8$^{+}$ donor T cells was determined for all organs by FACS analysis of CD8,

Thy1.1 and Thy1.2 expression after exclusion of host- and bone marrow-derived CD8$^+$ T cells, which expressed H-2K$^k$ and CD45.1 respectively (Figure 10B).
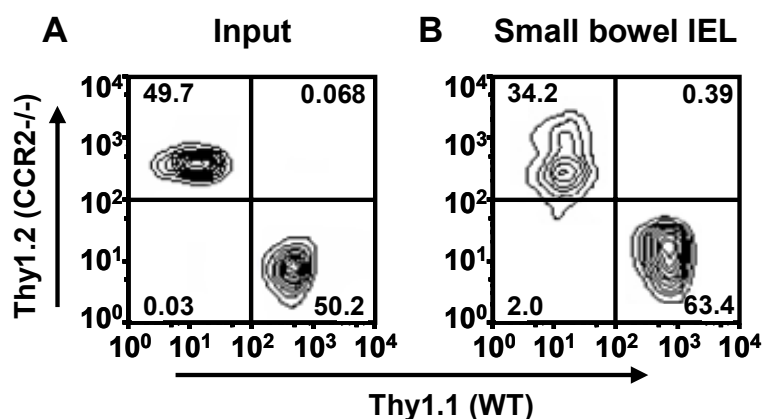


***Figure 10: FACS analysis of the competitive in vivo migration assay.***

*A) Equal numbers of WT (Thy1.1) and CCR2$^{-/-}$ (Thy1.2) CD8$^+$ T cells were mixed and accuracy of this procedure was determined by FACS analysis. B) Mixed WT and CCR2$^{-/-}$ CD8$^+$ T cells and TCD WT BM cells (CD45.1) were transplanted into lethally irradiated C3FeB6F1 recipients (H-2K$^k$) and distribution of WT and CCR2$^{-/-}$ CD8$^+$ T cells was determined on days 6, 14, and 28. This FACS density plot shows a day 6 sample of gut-infiltrating WT and CCR2$^{-/-}$ donor CD8$^+$ T cells after exclusion of host cells and bone marrow-derived cells. The percentage of infiltrating CCR2$^{-/-}$ CD8$^+$ T cells was reduced.*

The harvest time points chosen for analysis represent early alloreactive expansion in lymphoid organs, which begins in the first week after allogeneic BMT (149), and the subsequent migration and infiltration of GVHD target organs, which is most prominent between weeks 2 and 4 in this model (150). It was found that CCR2$^{-/-}$ CD8$^+$ T cells showed reduced infiltration of the liver as early as day 6 but differences were more prominent on days 14 and 28 (Figure 11B). Here, CCR2$^{-/-}$ CD8$^+$ T cells made up for only 32.6±3.6 % (day 14) and 37.8±7.3 % (day 28) of the infiltrate whereas WT CD8$^+$ T cells accounted for 67.4±3.6 % (day 14) and 62.2±7.3 % (day 28). The analysis of small bowel intraepithelial lymphocytes showed a migratory defect of CCR2$^{-/-}$ CD8$^+$ T cells for day 14 (60.5±1.9 % WT vs. 39.5±1.9 % CCR2$^{-/-}$) but not for days 6 and 28 (Figure 11A).
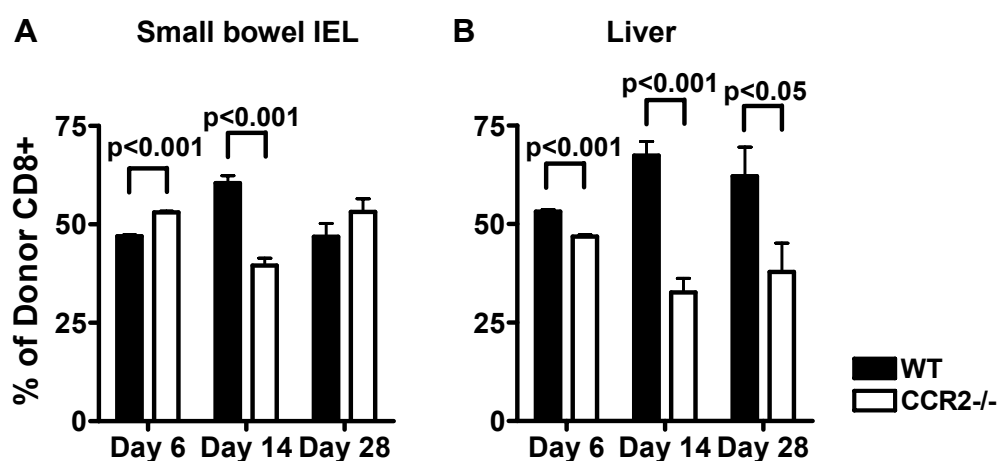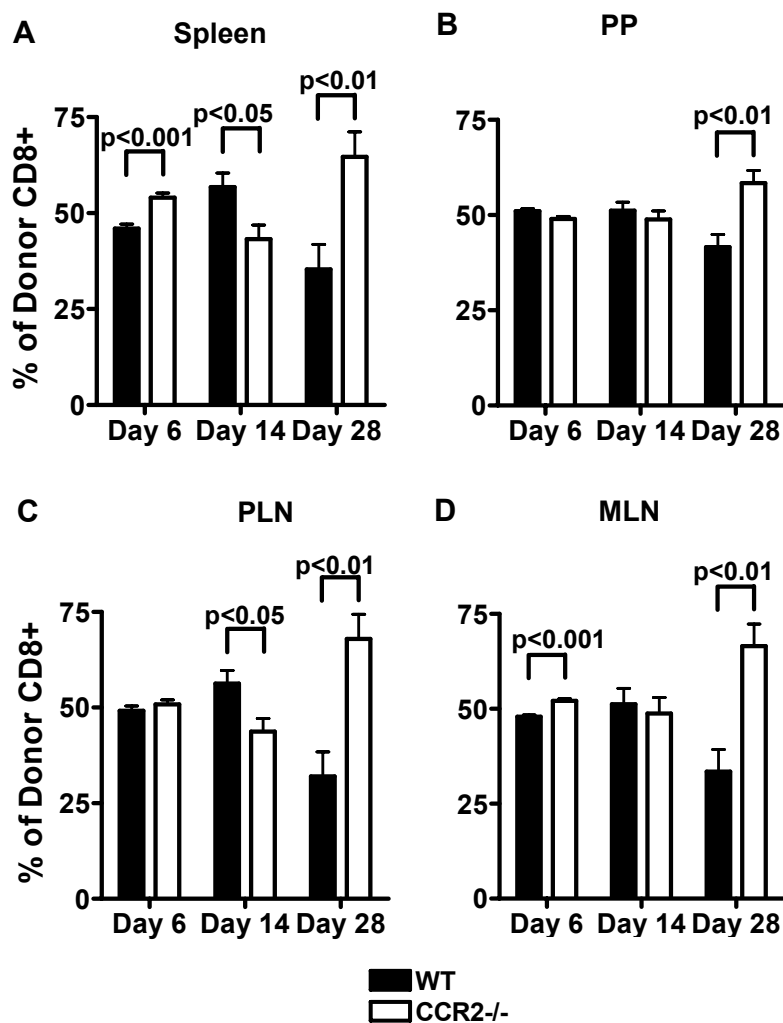
**Figure 11: Migration of CCR2$^{-/-}$ CD8$^{+}$ T cells into gut and liver during GVHD is reduced.**
*Lethally irradiated (1300 cGy) C3FeB6F1 mice received 5x10$^{6}$ TCD WT (CD45.1) BM cells together with a mix of 2x10$^{6}$ WT (Thy1.1) and 2x10$^{6}$ CCR2$^{-/-}$ (Thy1.2) CD8$^{+}$ T cells. Organs were harvested on days 6, 14, and 28 after BMT and analyzed by FACS. A) Small bowel IEL. B) Liver. Data represent the mean ± SEM of the percentage of infiltrating WT (■) or CCR2$^{-/-}$ (□) CD8$^{+}$ T cells of all donor CD8$^{+}$ T cells after exclusion of host- and BM-derived CD8$^{+}$ T cells. 8 mice in each group were analyzed per time point.*

Importantly, the initial accumulation (day 6) of CCR2$^{-/-}$ CD8$^{+}$ T cells in secondary lymphoid organs (spleen, PP, PLN, MLN) was not impaired (Figure 12A-D). Moreover, CCR2$^{-/-}$ CD8$^{+}$ T cells showed a prominent accumulation in secondary lymphoid organs on day 28, which corresponded to the decreased infiltration of the liver at this time point, and which might be due to selective trapping (spleen: 35.3±6.5 % WT vs. 64.7±6.5 % CCR2$^{-/-}$, PP: 41.6±3.3 %
WT vs. 58.4±3.3 % CCR2$^{-/-}$, PLN: 32.0±6.4 % WT vs. 68.0±6.4 % CCR2$^{-/-}$), MLN: 33.5±5.8 % WT vs. 66.5±5.85 % CCR2$^{-/-}$) (Figure 12A-D).

These results indicate that CCR2 is required for the migration of alloreactive donor CD8$^{+}$ T cells into the gut and liver during GVHD but is not required for the early migration into secondary lymphoid organs.

**Figure 12: Accumulation of CCR2$^{-/-}$ CD8$^+$ T cells in secondary lymphoid organs early after transplantation is intact. CCR2$^{-/-}$ CD8$^+$ T cells can be trapped in secondary lymphoid organs at later time points.**

*Lethally irradiated (1300 cGy) C3FeB6F1 mice received 5x10$^6$ TCD WT (CD45.1) BM cells with a mix of 2x10$^6$ WT (Thy1.1) and 2x10$^6$ CCR2$^{-/-}$ (Thy1.2) CD8$^+$ T cells. Organs were harvested on days 6, 14, and 28 after BMT and analyzed by FACS. A) Spleen. B) PP. C) PLN. D) MLN. Data represent the mean ± SEM of the percentage of infiltrating WT (■) or CCR2$^{-/-}$ (□) CD8$^+$ T cells of all donor CD8$^+$ T cells after exclusion of host- and BM-derived CD8$^+$ T cells. 8 mice per group were analyzed per time point.*

## 4.4  CCR2-deficient CD8$^+$ T cells have no functional defect besides impaired migration

To further clarify the role of CCR2 for the function of CD8$^+$ T cells and to test whether the reduced accumulation of CCR2$^{-/-}$ CD8$^+$ T cells in the gut and liver and the reduction of histopathological damage to these organs is due to any other defect besides reduced migration,
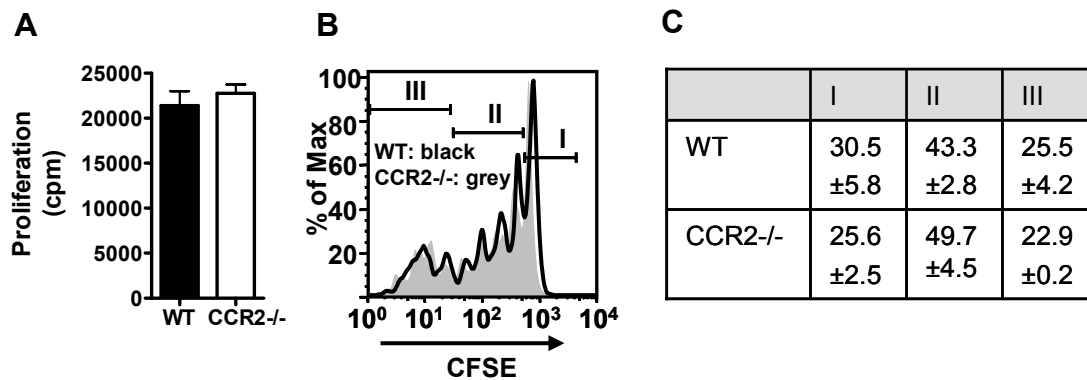
their proliferative response against alloantigens, the expression of activation markers after allostimulation, the production of cytokines and cytolytic activity were analyzed in a variety of *in vitro* and *in vivo* assays.

### 4.4.1  Alloreactive proliferation

First, a mixed lymphocyte reaction (MLR) was performed to detect any possible defects of CCR2$^{-/-}$ CD8$^{+}$ T cells in proliferation against alloantigens *in vitro*. WT and CCR2$^{-/-}$ CD8$^{+}$ T cells were incubated for 5 days with irradiated allogeneic C3FeB6F1 or BALB/c RBC-lysed splenic stimulators. Proliferation of effectors during the last 18 hours of incubation was measured via [$^{3}$H]thymidine incorporation. Background proliferation of stimulators and effectors alone was also measured and subtracted from values obtained for the MLR. No significant difference of *in vitro* proliferation of CCR2$^{-/-}$ CD8$^{+}$ T cells compared to WT CD8$^{+}$ T cells against C3FeB6F1 (Figure 13A) and BALB/c (data not shown) stimulators was found.

Second, proliferation against alloantigens was assessed *in vivo*. CFSE-labeled WT or CCR2$^{-/-}$ T cells were infused into sublethally (900 cGy) irradiated allogeneic C3FeB6F1 hosts. Proliferation kinetics was evaluated by FACS 72 hours after adoptive transfer (Fig 14B). Three separate populations of CFSE-labeled T cells in allogeneic recipients can be identified based on their rate of proliferation and the expression of cell surface activation markers (149). These populations consist of non-proliferative cells (high CFSE content and low or absent expression of activation markers, Figure 13B, population I), slow-proliferative cells undergoing homeostatic expansion (intermediate CFSE content and lack of activation markers, Figure 13B, population II), and fast-proliferative allo-activated T cells (low CFSE content and high expression of activation markers, Figure 13B, population III). Figure 13B shows histogram overlays of WT and CCR2$^{-/-}$ CD8$^{+}$ donor T cells, which demonstrate that CCR2$^{-/-}$ CD8$^{+}$ T cells have an intact alloproliferative response *in vivo*. Figure 13C shows the average values for all three populations for 4 mice.

**A**

**B**

**C**

| | I | II | III |
|------|------|------|------|
| WT | 30.5 ±5.8 | 43.3 ±2.8 | 25.5 ±4.2 |
| CCR2-/- | 25.6 ±2.5 | 49.7 ±4.5 | 22.9 ±0.2 |

*Figure 13: CCR2$^{-/-}$ CD8$^+$ T cells show intact proliferation against alloantigen.*

*A) MLR with WT and CCR2$^{-/-}$ CD8$^+$ T cell effectors and irradiated C3FeB6F1 stimulators. Bars represent mean ± SEM for specific proliferation of 12 replicate wells from one representative experiment out of three. cpm: Counts per minute. B), C) Sublethally irradiated (900 cGy) C3FeB6F1 mice received CFSE-labeled WT or CCR2$^{-/-}$ T cells. Recipient spleens were harvested after 72 hours for FACS analysis. B) Histogram overlays for CFSE-labeled WT (black line) and CCR2$^{-/-}$ (shaded area) donor CD8$^+$ T cells. Markers indicate non-proliferative cells (I), slow-proliferative cells (II), and fast-proliferative cells (III). Data shown are from one representative mouse out of four mice from two experiments. C) Mean ± SEM for all three populations for 4 mice.*

## 4.4.2  Upregulation of activation markers

CFSE-labeled T cells from the experiment in the previous figure were also stained for expression of the activation marker CD44, which is an adhesion molecule that is expressed at low levels by all hematopoietic cells and can be upregulated after TCR stimulation or exposure to inflammatory cytokines (151). It was found that CD44 is equally upregulated on fast-proliferative allo-activated WT and CCR2$^{-/-}$ CD8$^+$ T cells (Figure 14A). The same results were observed for CD25, which is the α-chain of the IL-2 receptor and therefore another valuable activation marker in GVHD (data not shown). These data were confirmed by examining the percentage of activated cells (CD44$^{hi}$CD62L$^{low}$ and CD25$^{hi}$CD62L$^{low}$) of all donor CD8$^+$ T cells in the spleen, gut, liver, MLN and PP of BMT recipients with GVHD (Figure 14B and data not shown).
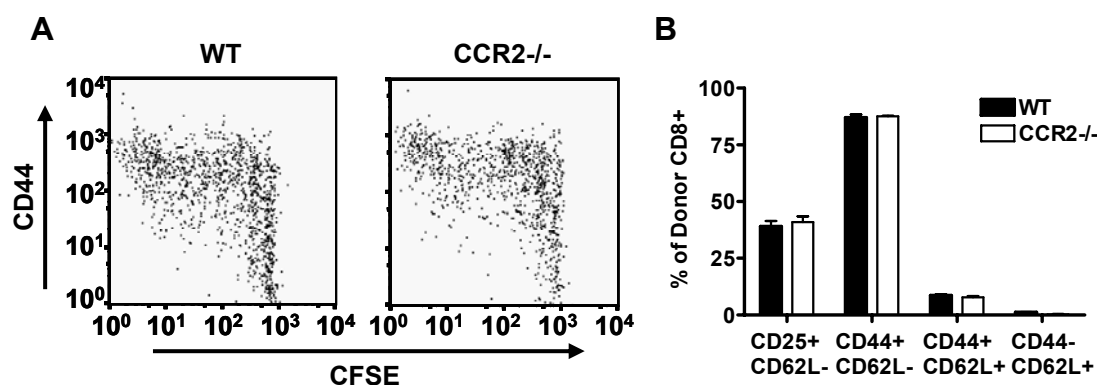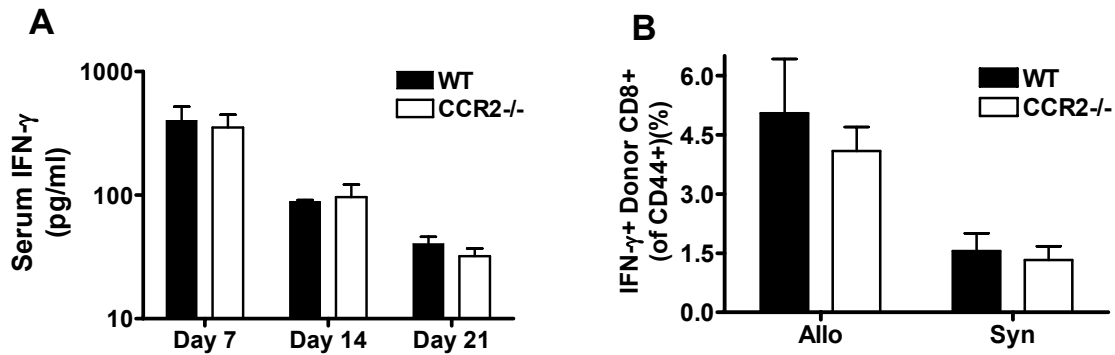
**Figure 14: CCR2$^{-/-}$ CD8$^+$ T cells have intact upregulation of activation markers.**

*A) Sublethally irradiated (900 cGy) C3FeB6F1 mice received CFSE-labeled WT or CCR2$^{-/-}$ T cells. Recipient spleens were harvested after 72 hours for FACS analysis. Dot plots of CFSE and CD44 expression on WT and CCR2$^{-/-}$ donor CD8$^+$ T cells. Data shown are from one representative mouse out of four mice from two experiments. B) Lethally irradiated (1300 cGy) C3FeB6F1 received 5x10$^6$ TCD WT BM cells in combination with 3x10$^6$ WT (■) or CCR2$^{-/-}$ (□) CD8$^+$ T cells. Recipient spleens were harvested at day 7 for FACS analysis of CD25, CD44, and CD62L expression. Shown is the mean ± SEM for 4 mice per group.*

### 4.4.3 Cytokine production

Earlier studies had found defects in Th$_1$ cytokine production in CCR2$^{-/-}$ mice during some inflammatory conditions (116, 118, 119, 126, 129, 152). IFN-γ is a central Th$_1$ cytokine and IFN-γ expression is usually high early after BMT (22). Therefore, serum IFN-γ levels were measured by ELISA in BMT recipients at days 7, 14, and 21 after transplant. No significant differences were observed between the two experimental groups (Figure 15A). As IFN-γ is mainly produced by donor T cells (22), this is a good indicator that IFN-γ production of CCR2$^{-/-}$ CD8$^+$ T cells is intact. Nevertheless, intracellular IFN-γ production of CCR2$^{-/-}$ CD8$^+$ T cells was also determined. Lethally irradiated C3FeB6F1 mice were transplanted with TCD WT BM together with WT or CCR2$^{-/-}$ CD8$^+$ T cells, spleens were harvested on day 7 after BMT and subsequently restimulated *in vitro* with irradiated TCD C3FeB6F1 splenic stimulators or syngeneic controls. Cytokine production was subsequently determined by ICC staining. Again, no difference in IFN-γ production was found between WT and CCR2$^{-/-}$ CD8$^+$ T cells (Figure 15B). Intracellular TNF-α expression was also similar for WT and CCR2$^{-/-}$ CD8$^+$ T cells but the expression levels observed were low (data not shown).
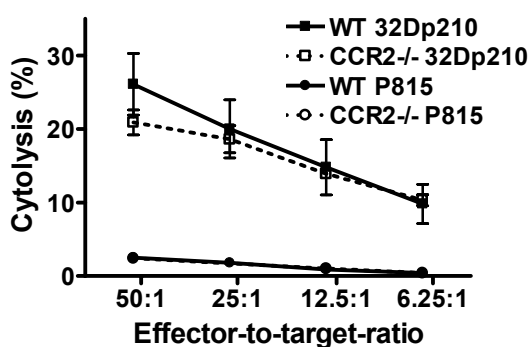
***Figure 15: CCR2<sup>-/-</sup> CD8<sup>+</sup> T cells have intact IFN-γ production.***

*Lethally irradiated (1300 cGy) C3FeB6F1 received $5x10^6$ TCD WT BM cells in combination with $3x10^6$ WT (■) or CCR2<sup>-/-</sup> (□) CD8<sup>+</sup> T cells. A) Serum cytokine levels were measured by ELISA at indicated time points. Shown is the mean ± SEM for 8-12 mice per group per time point. B) Recipient spleens were harvested at day 7 and restimulated for 12 hours with irradiated TCD C3FeB6F1 splenocytes. Cells were subsequently stained for intracellular IFN-γ. Shown is the mean ± SEM for 4 mice per group.*

### 4.4.4   Cytotoxicity

It was previously reported that CCR2<sup>-/-</sup> T cells might have a reduced cytolytic ability (152). Therefore, cytotoxicity of *in vivo*-activated CCR2<sup>-/-</sup> CD8<sup>+</sup> T cells was determined in a 4 hour $^{51}$Cr assay against the 32dp210 tumor cell line (C3H/He background) and a third party P815 control. No defect was observed for various effector-target-ratios (Figure 16).



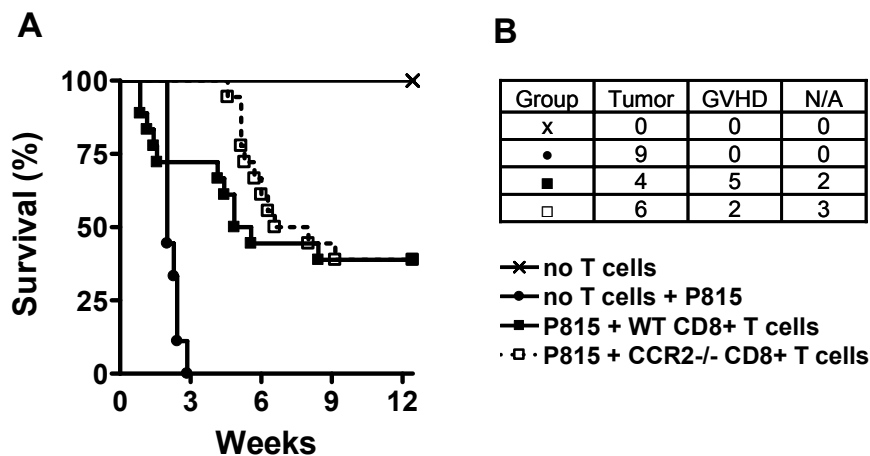***Figure 16: CCR2<sup>-/-</sup> CD8<sup>+</sup> T cells have intact cytotoxicity.***

*Lethally irradiated (1300 cGy) C3FeB6F1 received $5x10^6$ TCD WT BM cells in combination with $3x10^6$ WT (■) or CCR2<sup>-/-</sup> (□) CD8<sup>+</sup> T cells. Mice were sacrificed on day 7 and splenocytes were used as effectors in a $^{51}$Cr cytotoxicity assay. Targets were allogeneic 32Dp210 and third party P815. Shown is the mean specific lysis ± SEM for 4 mice per group.*

In summary, these functional tests indicate that the observed differences in morbidity, mortality, histopathology and organ infiltration are due to a migratory defect of alloreactive CCR2<sup>-/-</sup> CD8<sup>+</sup> T cells and not due to defects in proliferation, allo-activation, cytokine production or cytotoxicity.

## 4.5 CCR2-deficient CD8$^+$ T cells have intact graft-versus-tumor activity

Inhibition of GVHD without interfering with GVT activity is an important aim of any future therapeutic strategy in GVHD. Therefore, it was tested in a well-characterized GVHD/GVT model (B6→B6D2F1 with P815 mastocytoma) if CCR2-deficiency on donor CD8$^+$ T cells reduces GVHD but not GVT activity. Lethally irradiated B6D2F1 mice received allogeneic TCD BM alone or in a combination with WT or CCR2$^{-/-}$ CD8$^+$ T cells. Mice also received a dose of 1x10$^3$ P815 mastocytoma cells in a separate injection. Mice were monitored daily for survival and cause of death (tumor versus GVHD) was determined. Briefly, the presence of hind leg paralysis at the time of death or splenomegaly/liver metastases at the time of autopsy were used as specific criteria for death from tumor. Death from GVHD was defined as the absence of hepatosplenomegaly, the absence of leukemic cells on microscopic examination and the presence of GVHD symptoms.

It was found that the administration of P815 mastocytoma cells was lethal within 20 days for all mice that received TCD BM and no T cells. However, overall mortality was reduced to about 60% if WT CD8$^+$ T cells were added, which demonstrated the powerful anti-tumor effect of allogeneic donor T cells. Importantly, the addition of CCR2$^{-/-}$ CD8$^+$ T cells was able to rescue a similar proportion of BMT recipients, which suggests that GVT activity was completely preserved despite the absence of CCR2 signaling (Figure 17A).



| Group | Tumor | GVHD | N/A |
|-------|-------|------|-----|
| x | 0 | 0 | 0 |
| • | 9 | 0 | 0 |
| ■ | 4 | 5 | 2 |
| □ | 6 | 2 | 3 |

✕ no T cells
● no T cells + P815
■ P815 + WT CD8+ T cells
□ P815 + CCR2-/- CD8+ T cells

*Figure 17: The graft-versus-tumor activity of CCR2$^{-/-}$ CD8$^+$ T cells is intact.*

*B6D2F1 mice were lethally irradiated and subsequently received 5x10$^6$ TCD WT BM cells alone (x, n=9), TCD WT BM and 1x10$^3$ P815 mastocytoma cells (•, n=9) or TCD WT BM, 1x10$^3$ P815 mastocytoma cells and 3x10$^6$ WT (■, n=18) or CCR2$^{-/-}$ (□, n=18) CD8$^+$ T cells. Data represent two combined experiments. A) Kaplan-Meier survival curve. B) Cause of death. N/A: Not analyzed due to tissue necrosis.*

Of note, recipients of WT CD8^{+} T cells showed significant mortality due to GVHD early after transplant, whereas recipients of CCR2^{-/-} CD8^{+} T cells did not die from GVHD until week 6, which again demonstrated the reduced ability of CCR2^{-/-} CD8^{+} T cells to induce lethal GVHD (Figure 17).

Because the mice in the WT CD8^{+} T cell group that died early from GVHD could not be followed up for analysis of the GVT effect and because it was not always possible to clearly distinguish death from tumor and death from GVHD, *in vivo* bioluminescence imaging experiments with the newly established P815 TGL mastocytoma and A20 TGL lymphoma cell lines were performed. P815 TGL and A20 TGL were engineered to express the enzyme firefly luciferase, which catalyzes the oxidation of its substrate luciferin into non-reactive, non-toxic oxyluciferin and photons of light, therefore giving rise to a bioluminescence signal (153). Bioluminescence signals were quantified and visualized utilizing the low-light imaging system IVIS from Xenogen. The high sensitivity of BLI is shown in Figure 18 where an *in vitro* titration experiment was performed and as few as 100 cells could be visualized.
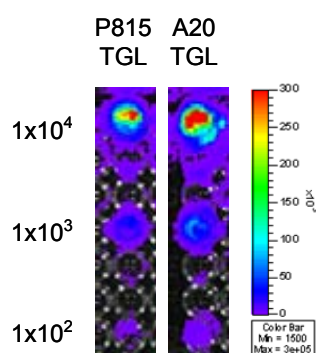


*Figure 18: P815 TGL and A20 TGL show bright bioluminescence.*
*$1x10^4$, $1x10^3$ and $1x10^2$ P815 TGL and A20 TGL cells were plated in complete RPMI in 96-well-plates. D-luciferin was added (150 µg/ml) and plates were imaged for 5 min using a Xenogen IVIS BLI system. Shown are pseudocolor images representing BLI intensity overlayed on conventional photographs. The color bar on the right indicates signal intensity measured in photons/sec/cm$^2$/sr.*

In BLI experiments, lethally irradiated B6D2F1 mice received allogeneic WT TCD BM alone or in combination with WT or CCR2^{-/-} CD8^{+} T cells. Mice also received a dose of $5x10^3$ P815 TGL mastocytoma cells in a separate injection. Mice were imaged at least once weekly over the course of four weeks. Figure 19A shows pseudocolor images of bioluminescence signal intensity overlaid on conventional photographs, and Figure 19B shows the time course of bioluminescence signal intensity. Both figures demonstrate that the GVT effect of CCR2^{-/-} CD8^{+} T cells is preserved. Similar results were obtained in a B6→BALB/c model with A20 TGL tumor cells (data not shown).

In summary, these results show that the GVT activity of CCR2^{-/-} CD8^{+} T cells is completely intact.
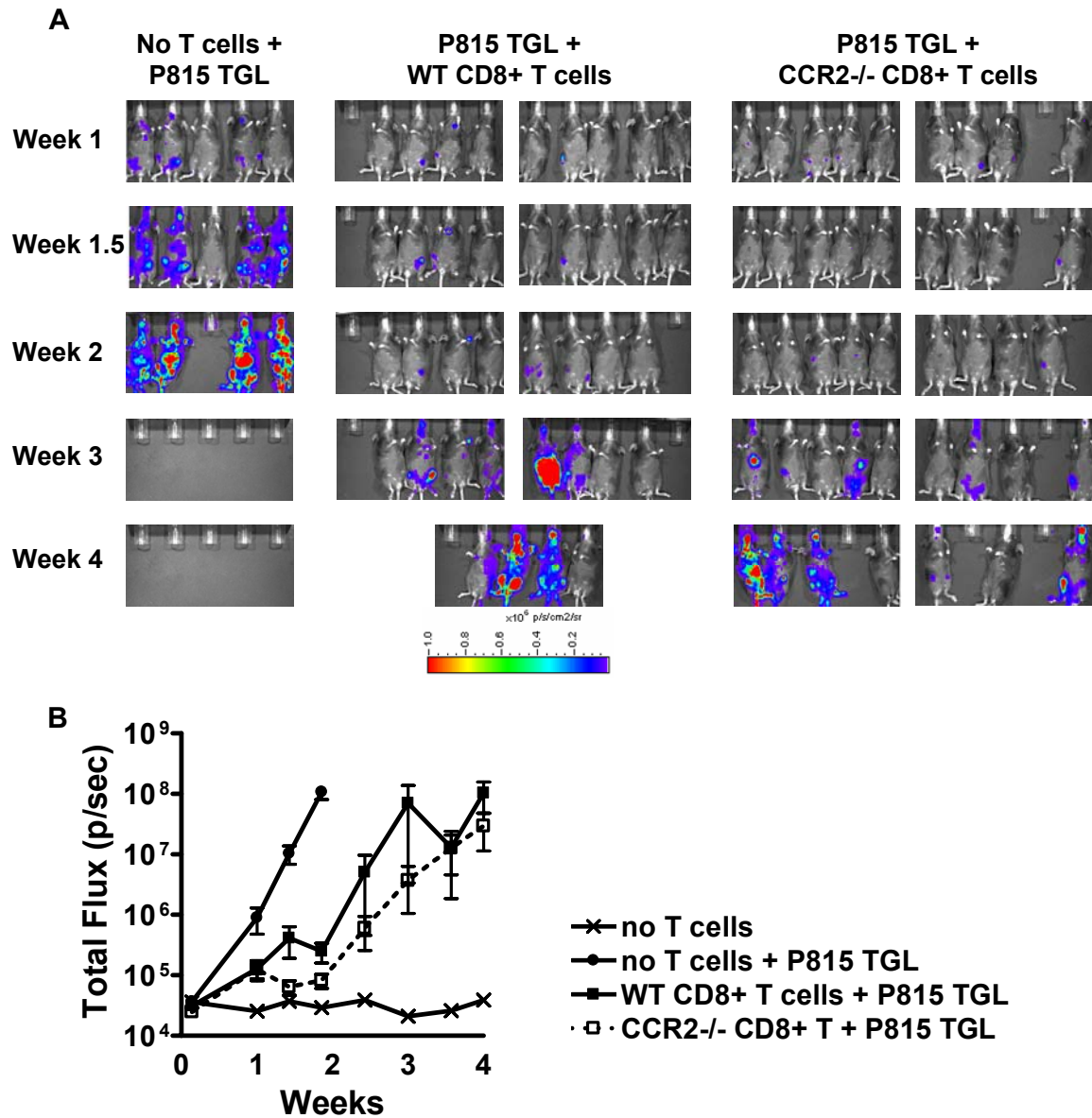
**Figure 19: The graft-versus-tumor activity of CCR2$^{-/-}$ CD8$^+$ T cells is intact.**

*B6D2F1 mice were lethally irradiated and subsequently received 5x10$^6$ TCD WT BM cells alone (x, n=5), TCD WT BM and 5x10$^3$ P815 TGL mastocytoma cells (•, n=5) or TCD WT BM, 5x10$^3$ P815 TGL mastocytoma cells and 3x10$^6$ WT (■, n=10) or CCR2$^{-/-}$ (□, n=10) CD8$^+$ T cells. A) Pseudocolor images representing whole body bioluminescence intensity overlaid on conventional photographs. B) Total flux in photons/sec/cm$^2$/sr. Mean ± SEM of all surviving mice is shown.*